

A NUMERICAL STUDY ON FORMATION OF THE NEGATIVE VORTICITY REGION OVER THE NORTHEAST SIDE OF THE QINGHAI-XIZANG PLATEAU*

WANG Yongqing (王咏青),

Nanjing Institute of Meteorology, Nanjing 210044

CHEN Lianshou (陈联寿)

Chinese Academy of Meteorological Sciences, Beijing 100081

and LUO Zhexian (罗哲贤)

Nanjing Institute of Meteorology, Nanjing 210044

Received April 29, 2001; revised April 5, 2002

ABSTRACT

In order to investigate the formation of the negative vorticity region over the northeast side of the Qinghai-Xizang (Tibetan) Plateau, four sets of numerical experiments have been performed in this paper with a quasigeostrophic barotropical model considering large-scale topography, diabatic heating and dissipation. The diabatic heating in the model contains a constant forcing and time-varying forcing. The time-varying characters are determined by the continuous evolution of the sensible heat flux at Damxung Station (30°29'N, 91°06'E) from 31 May to 4 June 1998. Results suggest that there are three types of processes significantly contributing to the formation of the negative vorticity region over the northeast side of the Qinghai-Xizang Plateau, and they are the advection of the anticyclonic vortex at the upstream by the basic flow, the energy dispersion of the cyclonic vortex over the south side of the Plateau, and the strengthening of anticyclonic systems produced by the thermal forcing of the Plateau.

Key words: TIPEX (Tibetan Plateau Experiment), Qinghai-Xizang (Tibetan) Plateau, vortex, thermal forcing, drought

I. INTRODUCTION

Advances in study on the effect of Qinghai-Xizang (Tibetan) Plateau on the synoptic-scale systems over its adjacent areas were made during the first Qinghai-Xizang Plateau Meteorological Science Experiment (QXPME), however those studies were generally limited to synoptic meteorology. As pointed by Yeh and Gao (1979), the detailed effects of the Plateau on synoptic systems remained to be studied.

What effects do the thermal forcing and topography of the Plateau have on the development of synoptic systems over its adjacent areas? What is the dynamic essence of

* This research was financially supported by the National Key Projects TIPEX and 973 China Heavy Rainfall.

the effects? Those are major problems we pay attention to during the second Tibetan Plateau Experiment (TIPEX) of Atmospheric Sciences, and this paper is going to present a part study result in this area.

II. TWO UNIQUE CLIMATIC PHENOMENA

It was found during the QXPMEX that, of the 218 warm lows from May to September in 1969–1976, 152 lows (accounting for 70%) have a small high to its north, and the two centers are approximately aligned on the same longitude (Su and Feng 1987), indicating that Plateau vortices often occur in pairs. The 500 hPa composite streamline field from 12 to 14 July 1970 (Fig. 1) shows this observational fact.

We used the NCEP/NCAR reanalysis data from May to August in 1992–1995 and 1998 to continue investigating the above fact. Daily 500 hPa streamline fields were first derived from the grid data of horizontal components (u, v) of winds. In the Plateau domain of 20–45°N and 70–105°E, with an altitude of more than 2000 m above sea level (hereafter asl for short), if a cyclonic center appeared, then a Plateau low was counted. Furthermore, if an anticyclonic center occurred simultaneously in the north of the cyclonic center in the above domain, then a pair of vortices was counted. Results show that, of 191 Plateau cyclonic vortices, 102 vortices (accounting for 53%) had an associated anticyclonic vortex in its north, which is comparatively in agreement with the result of the QXPMEX.

Therefore, it was preliminarily suggested that there often exist a pair of vortices in a dipole form of south-low-north-high at the 500 hPa level over the Qinghai-Xizang Plateau domain in summer. This may be a unique climatic phenomenon in the Plateau and its adjacent areas.

Based on the analysis of the annual rainfall data from 1951 to 1980, Bai and Xu (1988) pointed out that a dry tongue stretches southwards from the Ningxia Hui

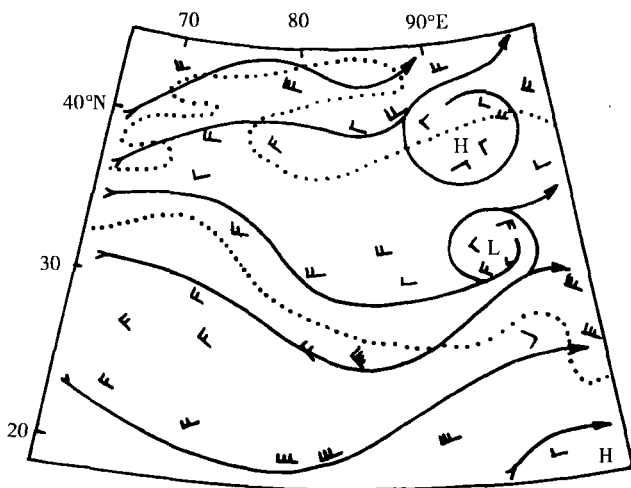


Fig. 1. The composite diagram of the 500 hPa streamline field for 12–14 July 1970 (from Su and Feng 1987). Dotted lines represent isolines of 2000 asl, and delineate the profile of the Plateau.

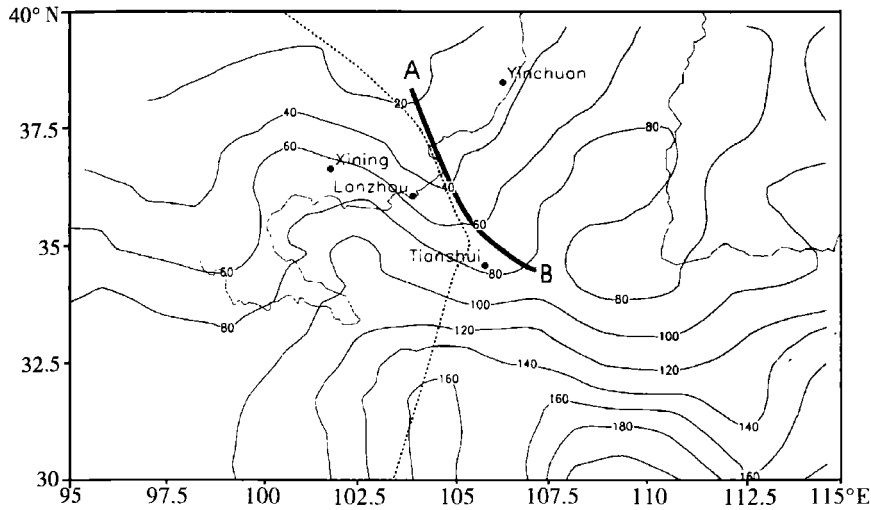


Fig. 2. Mean rainfall of May to August over 1951–1998 in northwest China. The units of isolines are mm. A thick line *AB* delineates the position of the dry tongue of rainfall. Dashed and dotted lines represent 2000 m asl and delineate the profile of the Plateau.

Autonomous Region to central Gansu Province, and this tongue corresponds to the negative vorticity area over the northeast side of the Qinghai-Xizang Plateau, resulting in the dry climate there.

The mean rainfall of May to August over 1951–1998 in northwest China (Fig. 2) was derived from the monthly rainfall data of 39 meteorological stations in the area of 30–40°N and 95–115°E. Shown in Fig. 2 is a clear dry tongue of rainfall over the northeast side of the Plateau. This may possibly be a unique climatic phenomenon in the rainfall distribution over the above area.

It is preliminarily inferred from the above that the formation of the negative relative vorticity region and the dry tongue of rainfall over the northeast side of the Plateau is associated with the eastward movement of the Plateau dipole of vortices. For this reason, we are going to analyze the possible dynamic connection between the above two unique climatic phenomena. Three aspects relating the formation of the negative relative vorticity region over the northeast side of the Plateau are analyzed, namely, the role of the anticyclonic vortices over the north Plateau, the role of the pairs of Plateau vortices and the influence of the thermal effect of the Plateau topography.

III. MODEL AND EXPERIMENT

A quasigeostrophic barotropic model (Charney and DeVore 1979) with large-scale topography, diabatic heating and dissipation was employed:

$$\frac{\partial}{\partial t} \nabla^2 \Psi + J(\Psi, \nabla^2 \Psi + f_0 \frac{h}{H} + \beta y) = -M \nabla^2 (\Psi - \Psi^*), \quad (1)$$

where Ψ is the geostrophic stream function, and J Jacobian operator. $f_0 = 2\Omega \sin\phi_0$, where

Ω is the rotation rate of earth, and φ_0 the latitude on the median of the β plane. $\beta = df/dy = 2\Omega \cos \varphi_0/a$, where a is the radius of earth. H is the depth of homogeneous atmosphere. $h(x, y)$ the height of topographic surface, and M the dissipation rate. $M\nabla^2\Psi^*$ is the thermal forcing term, and $-M\nabla^2\Psi$ the dissipation term.

Set

$$\Psi(x, y, t) = \bar{\Psi}(y) + \Psi'(x, y, t), \quad (2)$$

where $\bar{\Psi}(y)$ and $\Psi'(x, y, t)$ are the mean and perturbation stream functions respectively. $\bar{u}(y) = -d\bar{\Psi}/dy$ is the constant straight basic flow, and Ψ' the perturbation from the basic flow.

Substituting Eqs. (2) into (1) yields the perturbation stream function (hereafter " Ψ' " in Ψ' is omitted)

$$\frac{\partial}{\partial t} \nabla^2 \Psi + J(\Psi, \nabla^2 \Psi + f_0 \frac{h}{H} + \beta y) + \bar{u} \frac{\partial}{\partial x} \nabla^2 \Psi - \frac{d^2 \bar{u}}{dy^2} \frac{\partial \Psi}{\partial x} = -M \nabla^2 (\Psi - \Psi^*), \quad (3)$$

where $H=10$ km, $\varphi_0=30^\circ\text{N}$, $M=1.15 \times 10^{-6} \text{s}^{-1}$ and the corresponding e-fold rate is 10.1 days, which is close to that in the paper of Charney and DeVore (1979).

The computational domain is a square with its side being 4000 km, 401×401 grid points in total. $I=1, 2, \dots, 401$ successively increasing eastwards, and $J=1, 2, \dots, 401$ successively increasing northwards. At $J=201$, $\varphi=33^\circ\text{N}$. The grid spacing $d=\Delta x=\Delta y=10$ km, and the time step $\Delta t=5$ min. The value of $h(x, y)$ at grid points is determined by Exp. (4)

$$h(I, J) = \begin{cases} h_0 \sin \frac{I - I_{1h}}{I_{2h} - I_{1h}} \pi \sin \frac{J - J_{1h}}{J_{2h} - J_{1h}} \pi & (I_{1h} \leq I \leq I_{2h}, J_{1h} \leq J \leq J_{2h}), \\ 0 & (\text{other areas}). \end{cases} \quad (4)$$

The value $\bar{u}(J)$ of $\bar{u}(y)$ at grid points is specified by Exp. (5)

$$\bar{u}(J) = \begin{cases} \bar{u}_2 \sin \frac{J - 1}{J_{1u} - 1} \pi & (1 \leq J \leq J_{1u}), \\ \bar{u}_1 \sin(0.5 \frac{J - J_{1u}}{J_{2u} - J_{1u}} \pi) & (J_{1u} \leq J \leq J_{2u}), \\ \bar{u}_1 \sin(0.5 \frac{401 - J}{401 - 1} \pi) & (J_{2u} \leq J \leq 401). \end{cases} \quad (5)$$

The value of $\Psi^*(x, y)$ at grid points is given by Exp. (6)

$$\Psi^*(I, J) = \begin{cases} \Psi_0^* \sin \frac{I - I_{1s}}{I_{2s} - I_{1s}} \pi \sin \frac{J - J_{1s}}{J_{2s} - J_{1s}} \pi & (I_{1s} \leq I \leq I_{2s}, J_{1s} \leq J \leq J_{2s}), \\ 0 & (\text{other areas}). \end{cases} \quad (6)$$

In Exps. (4) - (6). $h_0=3$ km, $(I_{1h}, J_{1h}) = (41, 126)$, $(I_{2h}, J_{2h}) = (281, 276)$. The coordinates of the center of topographic surface $(I_h, J_h) = (161, 201)$, i. e. it is 400 km westwards from the center of the computational domain. $\bar{u}_2 = -5.0 \text{ m s}^{-1}$, $\bar{u}_1 = 10 \text{ m s}^{-1}$, $(J_{1u}, J_{2u}) = (135, 201)$, and this means that where is the straight east (west) wind, where is $\varphi < 24^\circ\text{N}$ ($\varphi > 24^\circ\text{N}$). $\Psi_0^* = 1.32 \times 10^7 \text{ m}^2 \text{ s}^{-1}$, which is reasonable in comparison with the value in the paper of Charney and DeVore (1979). $(I_{1s}, J_{1s}) = (161, 125)$, and

$(I_{2s}, J_{2s}) = (281, 201)$. The coordinates of the center of the heating area $(I_s, J_s) = (221, 163)$, i. e. it is 430 km southeastwards from the center of the computational domain.

With regard to the initial conditions, set the initial distribution of perturbation relative vorticity to be in a form of a pair of vortices:

$$\zeta(x, y, 0) = \zeta_s(x, y, 0) + \zeta_n(x, y, 0), \quad (7)$$

where ζ_s and ζ_n describe a cyclone and an anticyclone respectively

$$\zeta_s(x, y, 0) = \begin{cases} (2v_{ms}/R_m)(1.0 - 0.5(r_s/R_m))\exp(1.0 - (r_s/R_m)) & (r \leq r_0), \\ 0 & (r > r_0), \end{cases} \quad (8)$$

$$\zeta_n(x, y, 0) = \begin{cases} -(2v_{mn}/R_m)(1.0 - 0.5(r_n/R_m))\exp(1.0 - (r_n/R_m)) & (r \leq r_0), \\ 0 & (r > r_0). \end{cases} \quad (9)$$

where v_{ms} and v_{mn} are the maximum wind velocities of two vortices respectively. R_m is the radius of maximum wind, and r_0 the radius of vortices. $r_s = \sqrt{(x-x_{s0})^2 + (y-y_{s0})^2}$, $r_n = \sqrt{(x-x_{n0})^2 + (y-y_{n0})^2}$, (x_{s0}, y_{s0}) and (x_{n0}, y_{n0}) are the coordinates of the two centers of vortices, and their corresponding grid point coordinates are $(I_s, J_s) = (181, 171)$, $(I_n, J_n) = (181, 231)$.

As regard to the boundary conditions, the change rate of perturbation stream function is set to be zero, i. e. $\partial \Psi / \partial t = 0$ at the south and north boundaries, and the cycle boundary condition is used at the east and west boundaries. In comparison with the model in the paper of Charney and DeVore (1979), three explanations should be given:

The first, the grid spacing in the model of Charney and DeVore (1979) was 312.5 km. Since the horizontal scale of Plateau vortices is about 500 km, if the grid spacing is large, the structure of vortices can not be reasonably described. Therefore we set $d=10$ km.

The second, it was generally used in Charney and DeVore's paper and such kind of research that the thermal forcing is constant, i. e. the thermal forcing is only a function of space. It can be clearly seen from the intensive observation data of the sensible heat fluxes, effective long wave radiation and so on at Damxung Station during the TIPEX that the Plateau heating had a clear time-varying character (Fig. 3). The sensible heat, latent heat and so on at Gerze Station during the TIPEX also had a similar character (Liu and Hong 2000). The thermal forcing contains two parts: a constant part; and a time-varying

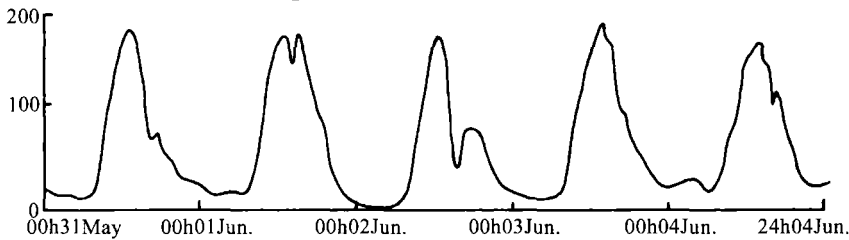


Fig. 3. The sensible heat flux curve at Damxung Station from 00 h 31 May to 24 h 4 June 1998. The abscissa represents time, and the ordinate the sensible heat flux in units of $W m^{-2}$.

one, i. e. $\Psi^*(x, y, t) = p(t)\Psi^*(x, y)$, where the temporal evolution of $p(t)$ is consistent with the curve in Fig. 3. It can be seen from Fig. 3 (omitted) in the paper of Liu and Hong (2000) that the phase of the transient curve of latent heat at Gerze Station is completely the same as that of sensible heat, and also consistent with Fig. 1 (omitted) in the paper of Miao et al. (1998). Meanwhile, the sum of sensible and latent heat is far greater than the effective longwave radiation, thus it is rational to take the time-varying pattern of the curve in Fig. 3 as the first approximation of $p(t)$.

The third, with regard to the size and intensity of initial vortices, there was a typical vortices pair process over the Plateau during 12–14 July 1970 (Fig. 1). We derived the stream fields and the maximum wind speeds of the two vortices from the wind data at 34 sounding stations in West China. The maximum wind speed of vortex over the southern Plateau was about 8.0 m s^{-1} , and that over the northern 5.6 m s^{-1} . The spatial scale of the two vortices was about 400 km, and the distance between the two centers of vortices was 600 km. The shape and intensity of initial vortices were determined on the basis of the above observational data, i. e. set $v_{ms} = 8.0 \text{ m s}^{-1}$ and $v_{mn} = 5.6 \text{ m s}^{-1}$ respectively in Eqs. (8) and (9), $R_m = 100 \text{ km}$, $r_0 = 200 \text{ km}$, $J_s = 171$, $J_n = 231$, the distance between the two centers $d = 600 \text{ km}$.

The integration time of four sets of experiments is 5 model days (Table 1). The distribution of initial perturbation relative vorticity for four experiments is given in Fig. 4.

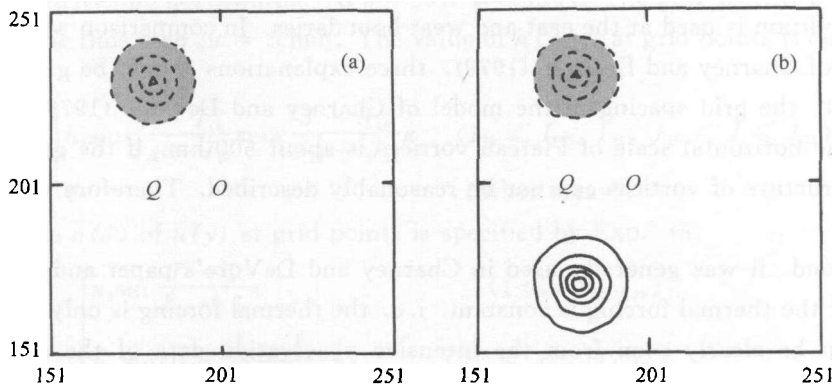


Fig. 4. The initial perturbation relative vorticity fields (a) for Experiment 1, and (b) for Experiments 2–4. The area of frame is $1000 \text{ km} \times 1000 \text{ km}$, and the computational domain is $4000 \text{ km} \times 4000 \text{ km}$. The figures on the edges of frame are grid point numbers, point O denotes the center of computational domain, point Q is the position of the mid-point between the two centers of vortices. The solid lines denote positive values, and the dashed lines negative values. The hatched region represents a negative relative vorticity area. The contour interval is $0.74 \times 10^{-4} \text{ s}^{-1}$.

IV. MAIN RESULTS

1. *Emergence of Negative Relative Vorticity Region over the Northeast Side of the Plateau due to the Eastward Movement of an Anticyclone over the Northern Plateau*

As stated above, there is often a negative relative vorticity region ranging southwards from the Ningxia Region to central Gansu Province on the northeast side of the Plateau. This is a synoptic and climatic background of the dry climate over the northeast side of the Plateau. For certain time period, if the negative vorticity region expands, then the drought could be more severe.

Table 1. A Brief Account of Experiments

Exp. No.	Max. altitude of topography	Basic flow	Plateau heating	Initial field
1	3 km	west wind north of 24°N	no heating	an anticyclone over the northern Plateau
2	3 km	west wind north of 24°N	no heating	vortice pair
3	3 km	west wind north of 24°N	constant heating	vortice pair
4	3 km	west wind north of 24°N	transient heating	vortice pair

In this paper we assign the region within 32 – 42°N and 100 – 110°E as the northeast side area of the Plateau, which is represented by a dashed line rectangle in Figs. 5–8. We assume that if the west basic flow advects anticyclones over the north side of the Plateau (near Qaidam Basin) downstream into the northeast side of the Plateau, then a negative vorticity region will appear in the northeast side. In order to confirm the assumption, Experiment 1 was conducted. After 36 h eastward movement, the anticyclone arrives at the west bound of the northeast side area (Fig. 5d), and stays in the area during 48–60 h (Figs. 5e–5f). Results of Experiment 1 show that the eastward movement of anticyclones over the north side of the Plateau may result in the emergence of negative vorticity region over the northeast side in some times, however the range of the negative vorticity area is limited and approximately equivalent to the scale of the anticyclonic vortex.

2. *The Eastward Movement of Vortice Pair Expands the Negative Vorticity Region over the Northeast Side of the Plateau*

As mentioned above, vortices over the Plateau often occurred in pairs, i. e. in a dipole form of south-low-north-high, this is a unique climatic phenomenon over the Plateau. The initial and boundary conditions in Experiment 2 are the same as those in Experiment 1 except that there is a cyclonic vortex south to the anticyclone over the north side of the Plateau in the initial field (Fig. 4b). By means of Experiment 2 we are going to analyze the effect of the eastward movement of a vortice pair on the genesis of negative vorticity over the northeast side. Results show that the circumstance of the eastward movement of a pair of vortices (Experiment 2) is quite different from that of a single anticyclone (Experiment

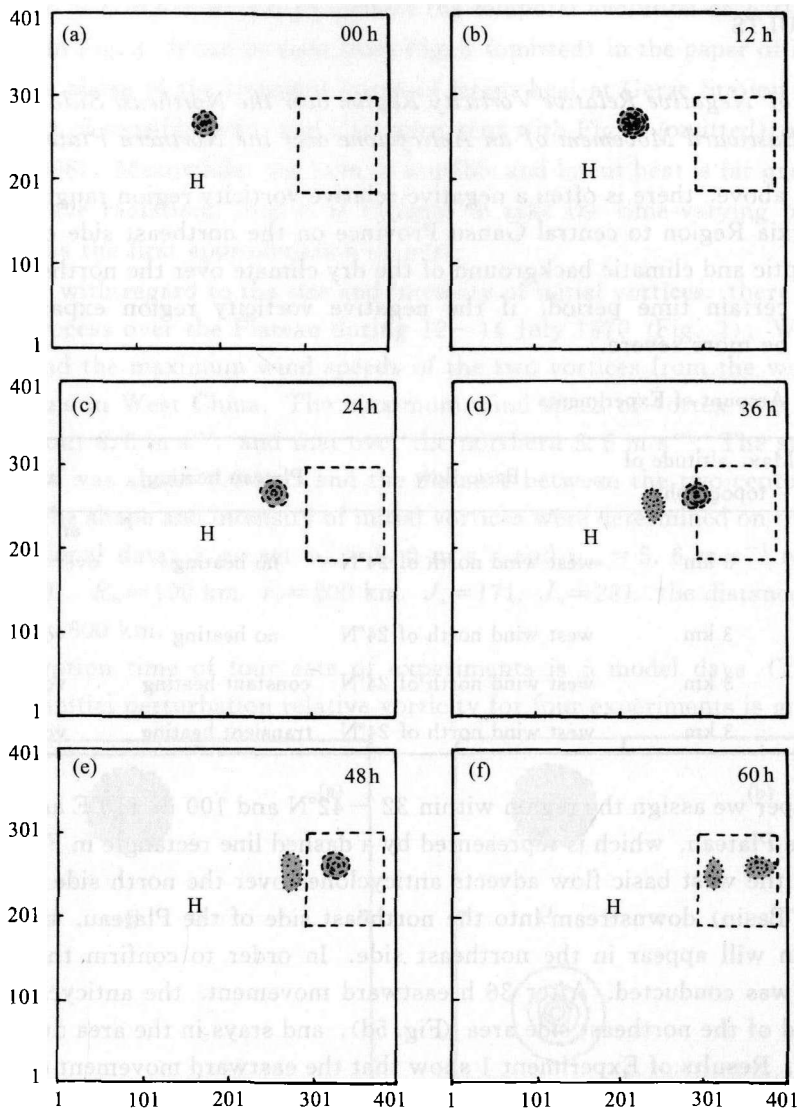


Fig. 5. Schematic diagram for the temporal evolution of the perturbation relative vorticity field in Experiment 1. H denotes the position of the center of the large-scale topography, and a dashed line rectangle the northeast side area of the Plateau. For the sake of clearness, only negative vorticity contours are plotted with the contour interval being $0.7 \times 10^{-4} \text{s}^{-1}$. The area of panel is $4000 \text{ km} \times 4000 \text{ km}$, and figures on its edges are grid point numbers.

1). At 12 h, there is a negative vorticity area (Fig. 6b) on the south side of the anticyclone. Afterwards, the negative vorticity area accompanies the anticyclonic vortex, and moves eastwards together (Fig. 6c). They both arrive at the west bound of the northeast side area at 36 h. In the period of 48–60 h, there appears a negative vorticity region over the northeast side area (Figs. 6e–6f), and the area of the negative vorticity region is far greater than its counterpart in Experiment 1 (Figs. 5e–5f). From the consideration of dynamics, the formation of negative vorticity region on the south or

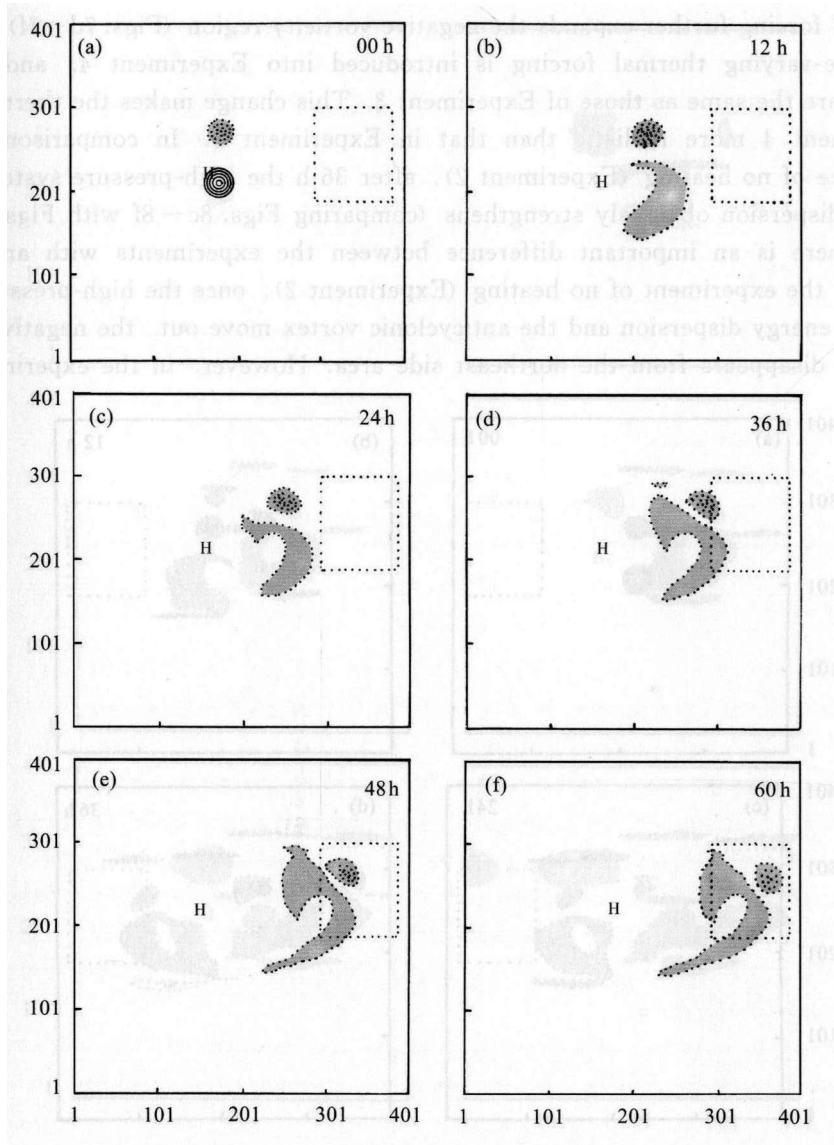


Fig. 6. As in Fig. 5 except for Experiment 2.

southwest side of the anticyclonic vortex arises from the energy dispersion from the cyclone on its south side. Xu et al. (1993) made a thorough investigation on the energy dispersion of the vortices on large-scale topography surface and the genesis of wavetrains. In addition, the formation may be associated with the interaction between vortex and basic flow, and this will be discussed in the other paper later.

3. Effect of Plateau Heating on the Negative Vorticity Region over the Northeast Side

The initial and boundary conditions of Experiment 3 are the same as those of Experiment 2 except that a constant Plateau heating is considered. In comparison of Experiments 2 and 3, we may analyze the effect of the thermal forcing on the formation of the negative vorticity region over the northeast side of the Plateau. Results display that

the thermal forcing further expands the negative vorticity region (Figs. 7d–7f).

A time-varying thermal forcing is introduced into Experiment 4, and its other conditions are the same as those of Experiment 3. This change makes the thermal forcing in Experiment 4 more realistic than that in Experiment 3. In comparison with the circumstance of no heating (Experiment 2), after 36 h the high-pressure system induced by energy dispersion obviously strengthens (comparing Figs. 8c–8f with Figs. 6c–6f). Besides, there is an important difference between the experiments with and without heating. In the experiment of no heating (Experiment 2), once the high-pressure system induced by energy dispersion and the anticyclonic vortex move out, the negative vorticity region also disappears from the northeast side area. However, in the experiments with

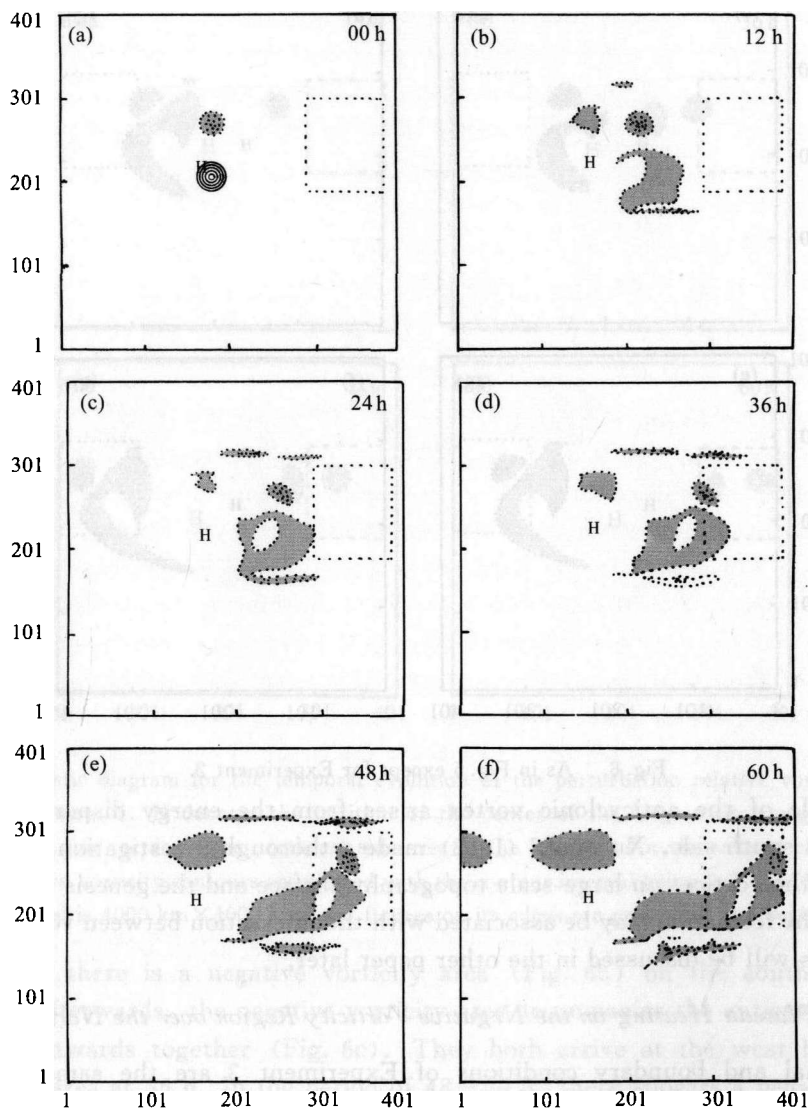


Fig. 7. As in Fig. 5 except for Experiment 3.

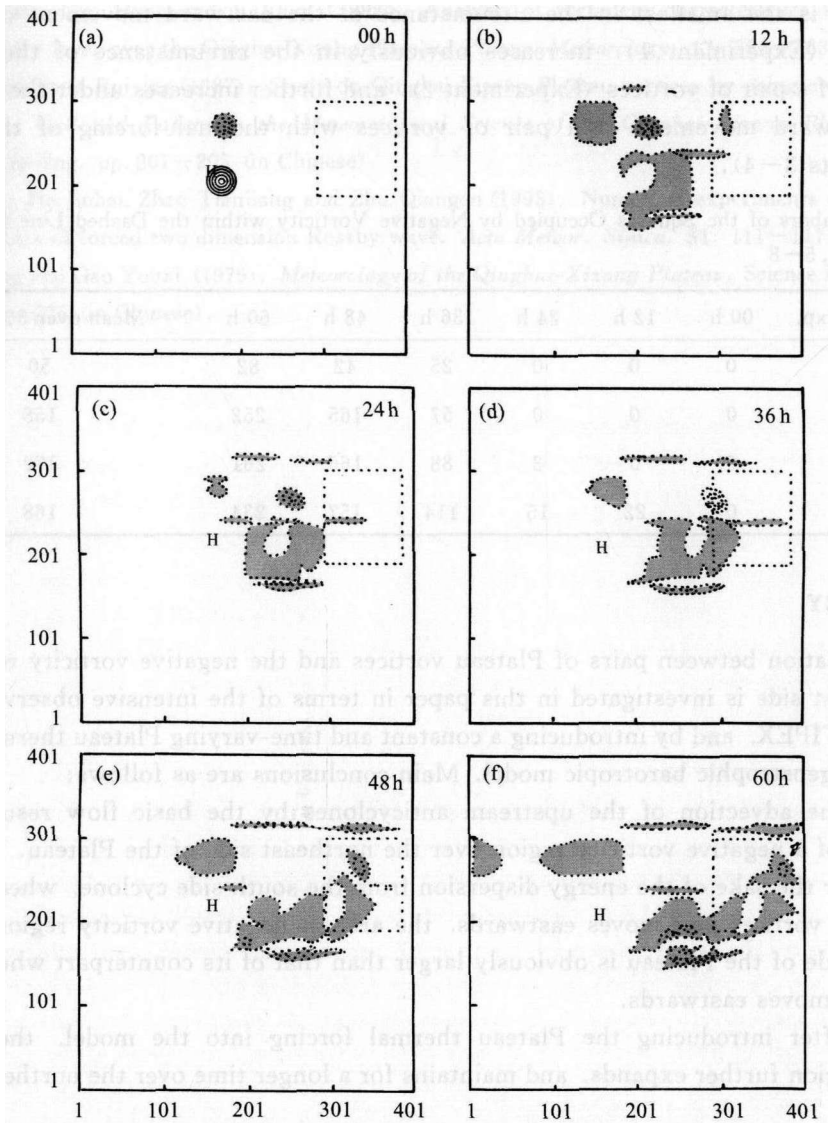


Fig. 8. As in Fig. 5 except for Experiment 4.

Plateau heating (Experiments 3 and 4), because the negative vorticity covers a large area in the upstream (Figs. 7d–7f; Figs. 8d–8f), the negative vorticity region can maintain over the northeast side area for a longer period after the anticyclonic vortex and the negative vorticity areas on its south side have moved out (figures omitted).

Results of Experiments 1–4 were further processed to give a quantitative description. The detailed processing procedures are as follows: at first the dashed line rectangle in Figs. 5–8 were divided into 598 small squares, then numbers of squares occupied by negative vorticity on the perturbation relative vorticity fields of the four Experiments at each time level were counted. The numbers may approximately describe the area of the negative vorticity region (Table 2). It is seen from the table that as far as the average over 36–60 h is concerned, the area of the negative vorticity region over the northeast side of

the Plateau is the smallest in the circumstance of the eastward movement of a single anticyclone (Experiment 1), increases obviously in the circumstance of the eastward movement of a pair of vortices (Experiment 2), and further increases under the conditions of the eastward movement of a pair of vortices with thermal forcing of the Plateau (Experiments 3–4).

Table 2. Numbers of the Squares Occupied by Negative Vorticity within the Dashed Line Rectangle in Figs. 5–8

Number of Exp.	00 h	12 h	24 h	36 h	48 h	60 h	Mean over 36–60 h
1	0	0	0	25	42	82	50
2	0	0	0	57	165	252	158
3	0	0	3	88	166	261	172
4	0	22	15	114	157	234	168

V. SUMMARY

The relation between pairs of Plateau vortices and the negative vorticity region over the northeast side is investigated in this paper in terms of the intensive observation data during the TIPEX, and by introducing a constant and time-varying Plateau thermal forcing into a quasigeostrophic barotropic model. Main conclusions are as follows:

(1) The advection of the upstream anticyclones by the basic flow results in the emergence of a negative vorticity region over the northeast side of the Plateau.

(2) For the sake of the energy dispersion from the south side cyclone, when a dipole-like plateau vortices pair moves eastwards, the area of negative vorticity region over the northeast side of the Plateau is obviously larger than that of its counterpart when a single anticyclone moves eastwards.

(3) After introducing the Plateau thermal forcing into the model, the negative vorticity region further expands, and maintains for a longer time over the northeast side of the Plateau.

The physical processes in the real atmosphere are highly complicated, the more complex mathematical and physical models are needed in the further study.

Acknowledgment: The third author would like to thank Prof. XU Xiangde for beneficial discussion on the numerical experiments of the physical processes in the Plateau earth-atmosphere system.

REFERENCES

- Bai Zhaoyi and Xu Guochang (1988). *Weather in Northwest China*. China Meteor. Press, Beijing, pp. 29–49 (in Chinese).
- Charney, J. G. and DeVore, J. G. (1979). Multiple flow equilibria in the atmosphere and blocking, *J. Atmos. Sci.*, **36**: 1205–1216.
- Liu Huizhi and Hong Zhongxiang (2000). Turbulent Characteristics in the surface layer over Gerze area. *Chinese. J. Atmos. Sci.*, **24**: 289–300 (in Chinese).

-
- Miao Manqian, Cao Hong and Ji Jijun (1998), Analysis of turbulent characteristics in atmospheric boundary layer over the Qinghai-Xizang Plateau. *Plateau Meteorology*, **17**: 356—363 (in Chinese).
- Su Binkai and Feng Ruiying (1987), Study on Qinghai-Xizang Plateau vortices by using energy spectrum analysis. *Collected Papers on the Meteorological Science of the Qinghai-Xizang Plateau*, Science Press, Beijing, pp. 201—205 (in Chinese).
- Xu Xiangde, He Jinhai, Zhao Tianliang and Zhu Qiangen (1993), Numerical experiments of propagation characters of forced two dimension Rossby wave. *Acta Meteor. Sinica*, **51**: 111—117 (in Chinese).
- Yeh Tuzheng and Gao Youxi (1979), *Meteorology of the Qinghai-Xizang Plateau*, Science Press, Beijing, pp. 267—275 (in Chinese).